

Distribution Agreement

In presenting this thesis or dissertation as a partial fulfillment of the requirements for an advanced degree from Emory University, I hereby grant to Emory University and its agents the non-exclusive license to archive, make accessible, and display my thesis or dissertation in whole or in part in all forms of media, now or hereafter known, including display on the world wide web. I understand that I may select some access restrictions as part of the online submission of this thesis or dissertation. I retain all ownership rights to the copyright of the thesis or dissertation. I also retain the right to use in future works (such as articles or books) all or part of this thesis or dissertations.

Signature:

Shagun Arora

Date

Analysis of Retinal Pigment Epithelium (RPE) Morphometry in Human Eyes

By

Shagun K. Arora, B.S.
Master of Science

Clinical Research

Hans Grossniklaus, M.D.
Advisor

Beau Bruce, M.D.
Committee Member

Mitch Klein, Ph.D.
Committee Member

Accepted:

Lisa A. Tedesco, Ph.D.
Dean of the James T. Laney School of Graduate Studies

Date

Analysis of Retinal Pigment Epithelium (RPE) Morphometry in Human Eyes

By

Shagun K. Arora
B.S., Emory University, 2009

Advisor: Hans Grossniklaus, M.D.

An abstract of
A thesis submitted to the Faculty of the
James T. Laney School of Graduate Studies of Emory University
in partial fulfillment of the requirements for the degree of
Master of Science
in Clinical Research
2014

Abstract

Analysis of Retinal Pigment Epithelium (RPE) Morphometry in Human Eyes

By Shagun K. Arora

Purpose: Describe RPE morphometry of normal human eyes with regard to age and topographic location. **Methods:** Cadaveric human donor eyes of varying ages were microdissected, RPE flatmounts were immunostained for AF635-phalloidin, nuclei stained by propidium iodide, and imaged by confocal microscopy. Image analysis was performed using ImageJ (NIH) and Cellprofiler software (Broad Institute, Cambridge, MA). A large number of quantitative parameters, including cell density, cell area, percentage of hexagonal cells, and measures of cell shape, were obtained from these analyses to characterize individual and groups of RPE cells. Measurements were taken from selected areas spanning the length of the retina, from the macula, mid-periphery, and far-periphery. **Results:** Fifteen eyes from 10 donors of varying ages ranging from 29-80 years were used. In the macula and far-periphery, an overall trend of decreasing RPE cell density, percent hexagonal cells and form factor was observed with increasing age. We also found a trend of increasing cell area and eccentricity with age in the macula and far-periphery. When individuals were divided into two age groups, <60 years old and ≥ 60 years old, there was a higher cell density, lower cell area, lower eccentricity and higher form factor in the younger group ($p < 0.05$ for all measurements). No significant differences in RPE morphometry between age groups were found in the mid-periphery. **Conclusions:** RPE cells become less dense, larger in size, lose their typical hexagonal shape and become more oval in shape with age.

Analysis of Retinal Pigment Epithelium (RPE) Morphometry in Human Eyes

By

Shagun K. Arora, B.S.
B.S., Emory University, 2009

Advisor: Hans Grossniklaus, M.D.

A thesis submitted to the Faculty of the
James T. Laney School of Graduate Studies of Emory University in partial
fulfillment of the requirements for the degree of
Master of Science
in Clinical Research
2014

Acknowledgments

This work was supported by the National Center for Advancing Translational Sciences of the National Institutes of Health under award numbers ULI TR000454 and TLI TR000456. This research was also supported under the following grants: NIH R01EY016470, R01EY021592, P30EY06360, an internal pilot grant from the Department of Neuroscience at Emory University, and an unrestricted grant to the Emory Eye Center from Research to Prevent Blindness, Inc. The content is solely the responsibility of the authors and does not necessarily represent the official views of the National Institutes of Health. Special thanks go to the Georgia and North Carolina Eye Banks.

Table of Contents

Introduction.....	1
Background.....	3
Methods.....	4
Results.....	8
Discussion/Conclusions.....	15
References.....	21
Tables and Figures	
Table 1: Summary of Past Studies.....	23
Figure 1: Study Population Diagram.....	25
Table 2: Donor Characteristics.....	26
Figure 2: Description of Methods.....	27
Figure 3: Image Selection.....	28
Figure 4: Image Analysis Technique.....	29
Table 3: Descriptive Statistics of RPE Morphometric Measurements.....	30
Figure 5: Correlation Analysis.....	31
Figure 6: Analysis of Spatial Variation of RPE Morphometry.....	32
Figure 7: Age-Related Morphometric Changes of RPE in 3	33
Areas of Retina	
Table 4: Average Morphometric Measurements Comparing	34
Patients <60 Years and \geq 60 Years of Age	
Figure 8: Representative Images of RPE Flatmounts.....	35
Table 5: Linear Regression Model Parameter Estimates.....	36

Introduction

The retinal pigment epithelium (RPE) is a metabolically active layer of the retina, which when damaged plays a key role in the pathogenesis of age-related macular degeneration (AMD) (1, 2). The normal structure of the RPE sheet has been described as a single monolayer of cells of hexagonal shape, forming a barrier between the neurosensory retina and the underlying choriocapillaris (3). This honeycomb appearance of this epithelium is known to be the most stable configuration of cells in nature (4). A hexagonal network of cells allows for the greatest coverage of area without cell overlap or empty area and with the least amount of surface tension (4). With this structure, cell-cell communication is maximized and the RPE is able to adequately nourish the overlying photoreceptors. Little is known about how the morphometry of RPE cells changes with normal aging. Understanding the normal aging process of RPE will better enable us to understand differences in age related retinal pathology.

Currently, RPE can be imaged *in vivo* with adaptive optics scanning laser ophthalmoscopy (AOSLO), an imaging technique used to measure living retinal cells (5). Preliminary studies show the instrument's ability to image individual photoreceptor and RPE cells in humans and rhesus macaques (6, 7), allowing for quantitative measurements of these retinal cells. Similar research of the cornea has allowed for morphometric measurements of corneal endothelial cells, which is now used for the clinical diagnosis of corneal pathology using specular microscopy (8).

In this study we describe normal changes in RPE morphometry that occur with age, establishing a baseline, which can be used to detect individuals who are outside the normal range. We aim to 1) estimate correlations that exist between measures of RPE

morphometry, including cell density, cell area, eccentricity, form factor and percent of hexagonal cells, 2) compare RPE morphometry in three areas of the retina; the macula, mid-periphery and far-periphery, 3) describe the association between age and measures of RPE morphometry, and 4) build a predictive model of “RPE age” using data acquired from this study.

Our study provides morphometric measurements that may be translatable to the clinical setting when combined with clinical imaging modalities. We hypothesize that with age, the RPE will become increasingly disorganized, with more pronounced changes in the macula, when compared to RPE of the mid-periphery and peripheral retina.

Background

Age-related loss of RPE cells has been reported in previous literature using a variety of methods (Table 1). A prior study by Panda-Jonas et al. reported a 0.3% decrease decline per year, and Del Priore et al. found a 0.23% rate of decline per year (9, 10). In contrast, other investigators, such as Watzke et al. and Harman et al., found no age-dependent changes in RPE cell density (11, 12). Previous studies by Ts'o and Friedman, and Dorey et al., which looked at different retinal regions, found that RPE cell density in the macula decreases with age (13, 14). Gao and Hollyfield concluded that the RPE declines at a rate of 14 RPE cells/mm² per year (15).

Investigators have also described changes in RPE cell density with relation to location in the retina. Several studies have found that RPE cell density decreases with increasing distance from the optic nerve (9, 10, 15). Gao and Hollyfield found foveal RPE cell density to be 63% higher than the periphery. Panda-Jonas et al. and Del Priore et al. also quantified RPE cell density in various areas of the retina. Del Priore et al. found macular RPE cell density to be 4980 ± 90 cells/mm².

Methods

Eye Tissue

Fifteen cadaveric normal human eye globes or posterior poles from ten donors of varying ages were obtained from the Georgia Eye Bank, Atlanta, GA and the North Carolina Eye Bank, Winston Salem, NC over a 3-year period from 2011 to 2013 (Figure 1). Eyes were considered for analysis if they were between the ages of 10 and 90 years old, if there was no documented history of ocular disease, no documented history of inherited or acquired retinal disease, and no apparent signs of chorioretinal pathology at the time of tissue processing. Eyes with prior cataract surgery or cataractous lenses were not excluded from the study. In an attempt to avoid samples with tissue degradation, eyes were excluded from the study if the time between death of the donor and preservation of the globe in fixative was known to be greater than 7 hours.

Tissue Processing

Upon arrival, eyes were immediately immersed in Z-fix (Anatech Ltd, Battle Creek, MI), a buffered zinc formalin fixative solution, for no more than 24 hours before being dissected. Whole eyes were dissected by dividing the globe superiorly and inferiorly, leaving a strip that included the optic nerve and extending to the ciliary bodies bilaterally (Figure 2A-B). The neurosensory retina was then carefully peeled off, leaving the remaining RPE, Bruch's membrane, and choroid (Figure 2C). The RPE and Bruch's membrane were removed from the choroid and flat-mounted onto a slide with a silicon barrier (Grace Bio-Labs, Bend, OR) (Figure 2D). Orientation of the tissue was maintained and noted. RPE flatmounts were immunostained with Alexa Fluor 635-

Phalloidin (Life Technologies, Grand Island, NY) to stain F-actin at the borders of the RPE cells and propidium iodide (Life Technologies, Grand Island, NY) to stain nuclei. The RPE was then imaged using a Nikon C1 confocal (Nikon, Tokyo, Japan) in a 15 μm thick stack and flat images were generated using maximum intensity projection using ImageJ with Bio-Formats tool (Figure 2E) (16, 17). Multiple images were photomerged using the Autopano Pro v2.5 software (Kolor, Montmélian, France) to create a composite image (Figure 2F). This method of dissection and staining resulted in images in which cell borders and nuclei were identified clearly.

Imaging and Data Collection

Image analysis was performed using the Cellprofiler software (Broad Institute, Cambridge, MA) (18). Measurements were taken from three zones spanning the length of the retina, corresponding to the macula, mid-periphery and far-periphery of the retina. (Figure 3). The macula was identified as being 3.0-3.5 mm away from the optic nerve and upon visual inspection of microscopic images and was deemed to be the area of tissue with the highest cellular density. By using consistent measurements between the three zones, we were able to reliably identify the macula, mid-periphery and far-periphery of the RPE. Three images 512x512 pixels in size were used from each zone for morphometric analysis. Cell borders were automatically traced and analyzed using the CellProfiler software (Figure 4A) providing several quantitative morphometric measurements. Five morphometric parameters were analyzed in this study: cell density, number of cell neighbors, cell area, eccentricity and form factor. Eccentricity, a measure of cell shape, gave us information about how elongated a cell was (Figure 4B). A perfect

circle has an eccentricity value of 0, while an oval has a larger eccentricity value approaching 1. Form factor measures how far a cell deviates from the shape of a perfect hexagon, taking into account that not all six-sided cells are equilateral hexagons (19) (Figure 4C). The form factor value is derived by taking the ratio of the cell's area to its perimeter². A cell that is a perfect equilateral hexagon has a form factor value of about 0.64, while less regularly shaped hexagons have a lower value. The analysis technique used in this study accurately measured several morphometric parameters of the RPE, allowing for the characterization of individual and groups of RPE cells of different ages.

Statistical Analysis

A univariate analysis was performed to provide descriptive statistics for each morphometric measurement. Next, associations between measurements were identified and analyzed using linear regression. To assess for spatial variation of RPE morphometric measurements between three areas of the retina, a one-way analysis of variance (ANOVA) test was performed. Linear regression analysis was used to estimate associations between RPE cell morphology and age in three areas of the retina. From this analysis, we estimated specific rates of changes that occur with age. We also divided our tissue samples into two groups: less than 60 years of age and greater than or equal to 60 years of age, with 60 being the age where retinal pathology such as AMD becomes more prevalent (20). We then compared measurements between the two age groups with a two-sided Student's t-test. Finally, a linear regression analysis was performed to develop a predictive model of age using the morphometric data from normal eyes acquired in this

study. This model could then be used to predict the “RPE age” of a patient relative to their actual age. A significance level of $p < 0.05$ was selected for all statistical tests

Results

Study Population

A total of 10 donors were used in this study ranging from 29 to 80 years old, with an average age of 58.8 years. 100% of donors were Caucasian and 60% of the donors were male. The most common cause of death was related to various advanced cancers. The death to preservation time was collected for 90% of the donors and ranged from 39 minutes to almost 7 hours, with an average death to preservation time of 4.31 hours (Table 2).

Univariate Analysis

Cell Density, measured in cells per mm^2 , and cell area, measured in μm^2 , both showed larger variation around the mean or median when compared to measurements such as eccentricity and form factor (Table 3).

Linear Regression Analysis

Linear regression showed a nearly perfect linear correlation between 1/average cell area and cell density ($r^2=0.99$) (Figure 5A). A strong negative correlation was observed between form factor and average eccentricity ($r^2=0.75$) (Figure 5B). A positive correlation was observed between average cell area and average eccentricity, and cell density and average form factor ($r^2= 0.70$ and 0.54 , respectively) (Figure 5C-D). A negative correlation was observed between cell density and average eccentricity, and average cell area and average form factor ($r^2= 0.62$ and 0.57 , respectively) (Figure E-F). No significant correlations were observed between the percentage of hexagonal cells and

the other measures of RPE morphometry ($r^2 < 0.2$ for all correlations).

Spatial Variation of RPE Morphometry

Average cell density was significantly higher in the macula (M= 4964.52, SD=1039.55) when compared to the mid-periphery (M= 3989.53, SD= 521.51) and far-periphery (M= 2521.22, SD= 907.88) (Table 3; Figure 6A; ANOVA $F(2, 39) = 29.21$, $p < 0.001$). Average cell area was significantly lower in the macula (M=182.06, SD= 86.72) when compared to the mid-periphery (M=215.39, SD=88.44) and far-periphery (M=328.62, SD=162.82; ANOVA, $F(2, 39) = 6.03$, $p = 0.005$; Figure 6B). Average eccentricity showed a trend towards a higher cellular eccentricity with increasing distance from the optic nerve ($p = 0.12$) (Figure 6C). Average form factor showed a trend towards a lower value with increasing distance from the optic nerve ($p = 0.71$) (Figure 6D). The percent of hexagonal cells did not show any discernible trend in relation to retinal location (ANOVA, $p = 0.62$) (Figure 6E). Post-hoc pair-wise comparisons of cell density using Tukey's HSD test showed significant pairwise comparisons between all pairs. Pair-wise comparisons were also significant between cell area in the mid-periphery and far-periphery, and macular cell area and cell area in the far-periphery.

RPE Morphology and Age: Macula

The average RPE cell density of a 512×512 pixel² image in the macula was 4964.52 cells/mm² (SD=1039.55). An overall trend of decreasing RPE cell density with age was seen in the macula ($r^2 = 0.32$, $p = 0.03$) (Figure 7A). We observed that the rate of decrease in the density of macular RPE cells was 0.54% per year. When individuals were divided

into two age groups, <60 years old and ≥ 60 years old, there was a higher cell density in the younger group when compared to the older group (Table 4, $p=0.03$). The average cell area of an RPE cell in the macula over all ages was $4652.36 \mu\text{m}^2$ ($\text{SD}=2216.19$). A trend of increasing average cell area with age was observed in the macula ($r^2= 0.34$, $p=0.02$) (Figure 7B). Cell area was also higher in the group with individuals ≥ 60 years of age (Table 4, $p=0.02$). Among all donors, the average percent of hexagonal RPE cells in the macula was 40%. The percent of hexagonal cells showed a decreasing trend with age ($r^2= 0.31$, $p=0.03$), and when older and younger groups were compared, the percent of hexagonal cells was higher in the younger group (Table 4, $p=0.01$) (Figure 7C). The average eccentricity of all macular RPE cells was 0.51 ($\text{SD}=0.16$). Average eccentricity showed a trend towards a higher value with increasing age ($r^2= 0.48$, $p=0.004$), and was higher in the older group, signifying that cells had a more elongated shape as they got older (Table 4, $p=0.01$) (Figure 7D). The average form factor value of macular RPE cells was 0.76 ($\text{SD}=0.09$) and displayed a decreasing trend with age ($r^2= 0.42$, $p=0.001$) and a lower average value in the older group, indicating that older cells were less symmetric in shape (Table 4, $p=0.03$) (Figure 7E).

RPE Morphology and Age: Mid-Periphery

The RPE cells of the mid-periphery were examined for age-dependent morphometric changes. Images used for analysis of the RPE of the mid-periphery were selected by measuring approximately 6.2-7.5 mm away from the macular region. Fourteen eyes from 10 donors of varying ages ranging from 29-80 years were used. Average cell density of RPE cells among all ages in a 512x512 pixel image of the mid-

periphery was 3989.53 cells/mm² (SD=521.51). The average area of RPE cells in the mid-periphery was 5504 μm² (SD=2259.96). Among all samples, the average percent of hexagonal cells was 38.51%. The average eccentricity was 0.55 (SD=0.15) and the average form factor was 0.75 (SD=0.08). There was minimal correlation between any of the morphometric parameters and age (Figure 7, $r^2 < 0.21$ and $p > 0.05$ for all measurements). When individuals were divided into two age groups, <60 years old and ≥60 years old, there were no significant differences between the younger and older groups in any of the measured morphometric parameters (Table 4, $p > 0.05$ for all measurements).

RPE Morphology and Age: Far-Periphery

RPE cells from the far-periphery of the retina were analyzed. Images used for analysis of the RPE of the far-periphery were selected by measuring a total distance of approximately 13.7 to 16.2 mm away from the macular region. Fourteen eyes from 9 donors of varying ages ranging from 29-80 years old were used. The average RPE cell density of a 512x512 pixel² image in the far-periphery was 2521.22 cells/mm² (SD=907.88). An overall trend of decreasing RPE cell density with age was seen in the far-periphery ($r^2 = 0.45$, $p = 0.001$) (Figure 7A). We observed that the rate of decrease in the density of RPE cells in the far-periphery was 0.94% per year. When individuals were divided into two age groups, <60 years old and ≥60 years old, there was a higher cell density in the younger group (Table 4, $p = 0.02$). The average cell area for RPE cells in the far-periphery was 8397.82 μm² (SD=4160.66). A trend of increasing average cell area with age was observed in the far-periphery ($r^2 = 0.40$, $p = 0.01$) (Figure 7B). Cell area was

higher in the older group (Table 4, $p=0.02$). Among all samples, the average percent of hexagonal RPE cells in the far-periphery was 39.40 percent. The percent of hexagonal cells showed a minimal association with age ($r^2= 0.05$, $p=0.43$), and when older and younger groups were compared, the percent of hexagonal cells was not significantly different than the younger group (Table 4, $p=0.26$) (Figure 7C). The average eccentricity of RPE cells in the far-periphery was 0.63 (SD=0.05). Average eccentricity showed a trend towards a higher value and a more elongated shape with age ($r^2= 0.51$, $p=0.004$), and was higher in the older group (Table 4, $p=0.01$) (Figure 7D). Form factor had an average value of 0.74 (SD=0.08) and displayed a decreasing trend with age ($r^2= 0.48$, $p=0.006$) and a lower average value in the older group (Table 4, $p=0.01$) (Figure 7E).

Representative images comparing a younger individual (37 years) to an older individual (75 years) clearly show changes in RPE morphometry. The older individual displays a decreased cell density, increased cell area, and a loss of the uniform hexagonal epithelium in all three areas of the retina, corresponding to the morphometric measurements reported earlier (Figure 8). These images also show increasing cell disorganization and a more irregular cell shape in both the young and old individual with increasing distance from the optic nerve. We observed numerous clusters of cells with one central pyknotic cell surrounded by 5-6 larger cells, which were migrating towards the central cell. These structures are referred to as “cellular rosettes” (21).

Model of “RPE age”

A linear regression analysis was performed on the data to establish a predictive model with which an “RPE age” of a given clinical subject could be calculated. The

“RPE age” could be used to assess whether a subject’s RPE appears to be older or younger than the subject’s actual age. For example, suppose a 55-year-old subject were to have their RPE scanned *in vivo* using AOSLO and it was found that their RPE morphometry predicted their RPE age to be 65. The predictors used in this model included average cell density, cell area, eccentricity, form factor and percent hexagonal cells:

x_1 = average cell density

x_2 = average cell area

x_3 = average eccentricity

x_4 = average form factor

x_5 = average percentage of hexagonal cells

Data from the macula was used to build this model in Statistical Analysis Software (SAS). The macula was chosen because the macula was the only area of the retina that showed significant variability among subjects of different ages for all morphometric measurements. All morphometric measures were found to be significant predictors of the RPE age ($p < 0.001$) and were included in the model. The overall F-test of the regression model was found to be significant, with a test statistic value of 2779.65 and a p-value of < 0.001 .

Estimate of the final model:

$$\hat{Y} = \hat{\beta}_0 + \hat{\beta}_1 X_1 + \hat{\beta}_2 X_2 + \hat{\beta}_3 X_3 + \hat{\beta}_4 X_4 + \hat{\beta}_5 X_5 + E$$

$$\hat{Y} = \text{RPE Age}$$

$$\hat{\beta}_0 = 133.22$$

$$\hat{\beta}_1 = -0.01$$

$$\hat{\beta}_2 = -0.02$$

$$\hat{\beta}_3 = 74.14$$

$$\hat{\beta}_4 = -55.15$$

$$\hat{\beta}_5 = 2.99$$

E= error

Model parameter estimates and overall statistical measures are shown in Table 5. The median of the 95% prediction interval for the model was 57.51 years, suggesting that for future observations, this model can estimate age within ~29 years with 95% confidence.

Discussion / Conclusions

Although age-related loss of RPE cells has been reported in the literature, to our knowledge the details surrounding exactly how the shape of RPE cells change with age have not been investigated. Our study confirms the conclusions of previous investigations that there is an overall age-related decline in RPE cell-density. We found a 0.45% decrease in overall RPE cell density per year, a slightly higher rate of decline than the previous findings of Panda-Jonas et al. and Del Priore et al, who found a 0.3% and 0.23% rate of decline per year, respectively (Table 1) (9, 10). While most previous studies looked at small portions of the retina, our study investigated RPE cell morphometry from a continuous strip of tissue including three different zones of the retina: the macula, mid-periphery and far-periphery. Previous studies by Ts'o and Friedman, and Dorey et al. confirm our findings that RPE cell density in the macula decreases with age (13, 14). However in contrast to these two studies, our study found a significant decrease in RPE cell density with age in the peripheral retina as well. We found that the average rate of peripheral RPE cell loss was about 32 cells/mm² per year, while research by Gao and Hollyfield concluded a lower rate of decline at 14 RPE cells/mm² per year (15).

Gao and Hollyfield, Panda-Jonas et al. and Del Priore et al., all confirmed our finding that RPE cell density decreases with increasing distance from the optic nerve. Gao and Hollyfield found foveal RPE cell density to be 63% higher than in the periphery, while our study found macular RPE cell density to be about 97% higher than the periphery. As we did in our study, Panda-Jonas et al. and Del Priore et al. also quantified RPE cell density in various areas of the retina. Del Priore et al. found macular RPE cell

density to be 4980 ± 90 cells/mm², which is very similar to our finding of 4964.52 cells/mm².

The substantial variability in the data reported in the literature can partly be explained by vast differences in the methods used between investigators. Each of the previous studies used different methods to sample various areas of the retina, making the quantitative measurements virtually incomparable between studies. Furthermore, there can be great variability within a study, emphasizing the importance of sampling the same location relative to the optic nerve in each eye (11). Many of the previous studies also measured RPE cell density by simply counting the number of stained nuclei present. This method can be inaccurate and falsely overestimate cell density, because we observed in our images that many RPE cells are multinucleate. For this reason, we assessed cell density by automatically outlining cell borders and counting whole cells, rather than nuclei.

Additionally, many earlier studies have used sectioned or bleached tissues for their analyses, yielding low-quality images to obtain cell counts. In some more recent studies, RPE cells have been imaged with greater resolution due to improvements in imaging techniques. Our study is the first to use imaging methods that are clinically translatable and automated. We imaged RPE cells using confocal microscopy, an imaging technique that uses similar technology as AOSLO, which can be used to image individual RPE cells *in vivo*. We believe our methods, which use an advanced imaging technique and an automated image analysis software, can be easily translated to the clinical setting for detection of early subclinical retinal pathology. In retinal diseases such as AMD, RPE remodeling occurs much before the appearance of clinical manifestations of disease such

as drusen deposition, choroidal neovascularization and the accumulation of residual bodies that contain lipofuscin (22). It is believed that as the RPE cells age, an increasing toxic burden causes RPE cells to enter a state of cell senescence. In this state, the RPE cells are no longer able to perform their normal functions, leading to accumulation of debris and drusen in the cells (23). We believe that as RPE cells enter this stage of senescence, their morphology will change and that this age-related change is detectable by the methods proposed in our study.

Our study found that RPE cell morphometry changes with age in the macula and far-periphery, but not in the mid-periphery. We concluded that RPE cells in the macula and far-periphery become less numerous, larger in size, more elongated in shape and less hexagonal with increasing age. These changes were likely observed in the macula because there is greatest cell turnover in this area of the retina. The macula is highly metabolically active, which causes a buildup of toxic waste over time. With increasing age, this toxic burden eventually becomes excessive, leading to age-related degenerative changes, such as soft drusen, basal laminar deposits and calcification of Bruch's membrane (11). These changes damage the integrity of RPE cells over time and ultimately lead to cell death (24). The mid-periphery of the retina, however, seems to be relatively protected from these age-related changes perhaps because it is a generally stable area of the retina where not much light damage occurs (25). Also, RPE cell migration of peripheral RPE cells may help compensate for the death of cells in the mid-periphery, masking any age-related changes. The far-periphery of the retina shows age-related changes in RPE morphometry possibly caused by retinal and RPE thinning that may be worsened with increasing age (24). It is also thought that the far-periphery may

be more likely to be remodeled because of the presence of RPE stem cells in the marginal zone region of the ciliary body of some species (26, 27).

Our findings suggest that with the gradual loss of RPE cells, existing RPE cells become larger to fill in the empty spaces left behind by dying cells. This mechanism preserves the overall stability and integrity of the RPE monolayer. We observed numerous manifestations of this process in the form of cellular rosettes. These clusters of cells appeared as one central pyknotic cell surrounded by 5-6 larger cells, which were migrating towards the central cell. The surrounding cells appeared to be more stretched and elongated in shape, explaining our observation of increased average cellular eccentricity with older age (21). Prompt detection of these structures may serve as an early diagnostic method for retinal pathologies that involve RPE cell death.

We also found significant spatial differences in RPE cell density and cell area. In agreement with previous studies, we observed that RPE cells become less dense and larger in size with increasing distance from the optic nerve (10). The higher density of RPE cells in the macular region may be necessary to support the requirements of the retina and increased cone density. One hypothesis is that the smaller cell surface area is offset by a thicker RPE cell of the same volume. This packing of subcellular components in a taller elongated column may allow more RPE-specific activities in a higher density. We also found that RPE cells become less regular in shape in the periphery. The regular shape of the cells in the macular region suggests that there are no external forces causing irregular tension on the cells. On the other hand, the more irregularly shaped peripheral RPE cells may be subject to forces causing irregular tension on the cells.

One pitfall of this pilot study is the relatively low sample size that was used, causing an increased observed variability in measurements between donors. While this variability in morphometric measurements was expected due to normal differences in degrees of physiologic aging, a larger sample size would have helped to reduce variability to better reflect the population. Furthermore, our “RPE age” model suffered from our low sample size making it ineffective at predicting age with any certainty at this pilot stage. Because this study was a pilot study, we were not able to determine the sample size needed for sufficient power prior at the start of the study. Variability in measurements was limited with the use of automated image analysis software. Individual images used for analysis were handpicked and excluded from the study if they were of low quality. We assessed the accuracy of the software by comparing data from hand-traced images to data from CellProfiler. We found that the automated tracing done by the software was accurate, reproducible, and a much quicker method of image analysis that produced instant data. We also demonstrated the integrity of our data using this method by showing a perfect linear correlation between $1/\text{average cell area}$ and cell density and a strong negative correlation between average form factor and average eccentricity. The sample of donors used in this study encompasses an age range of 51 years and a fairly even sex distribution, generalizable to most populations of interest. Cancer was the most common cause of death of donors in this study set, also representative of the United States population (28). The average death to preservation time of less than 7 hours ensured that the tissue used in this study had minimal autolytic changes (29).

In the future, as we anticipate improvements in AOSLO imaging of RPE cells, we plan to repeat these experiments with larger populations using AOSLO images. We also

plan to describe RPE morphometry in early and late stages of AMD to assess whether the normal changes of aging found in this study resemble those in AMD.

Significant age-dependent changes were seen in the RPE morphometry of the normal aging eye. RPE cell density in the macula, percent of hexagonal cells and average form factor showed a decreasing trend with age, while the average cell area and eccentricity showed an increasing trend. The RPE cells also lost their typical hexagonal shape and became more elongated. These observed differences in the aging eye may resemble early changes seen in the pathologic RPE of AMD. This study proved that changes seen with age and location of the retina can be visibly detected, indicating that as clinical RPE imaging is perfected, such as AOSLO, our findings may provide a baseline for normal RPE morphometric aging in these images. Data from this study can be used to detect individuals who fall out of the norm, thus prompting clinicians to watch these patients closely for possible progression to retinal pathology and recommend early intervention therapies such as AREDS vitamins enrichment or other treatments(30).

REFERENCES

1. Ehrlich R, Harris A, Kheradiya NS, et al. Age-related macular degeneration and the aging eye. *Clinical interventions in aging* 2008;3(3):473-82.
2. Liang FQ, Godley BF. Oxidative stress-induced mitochondrial DNA damage in human retinal pigment epithelial cells: a possible mechanism for RPE aging and age-related macular degeneration. *Experimental eye research* 2003;76(4):397-403.
3. Foulds WS. The retinal-pigment epithelial interface. *The British journal of ophthalmology* 1979;63(2):71-84.
4. Thompson DAW. 1966. In: Bonner J, ed. *On Growth and From*. Cambridge: University Press, 1965:88-131.
5. Roorda A. Applications of adaptive optics scanning laser ophthalmoscopy. *Optometry and vision science : official publication of the American Academy of Optometry* 2010;87(4):260-8.
6. Morgan JI, Dubra A, Wolfe R, et al. In vivo autofluorescence imaging of the human and macaque retinal pigment epithelial cell mosaic. *Investigative ophthalmology & visual science* 2009;50(3):1350-9.
7. Roorda A, Zhang Y, Duncan JL. High-resolution in vivo imaging of the RPE mosaic in eyes with retinal disease. *Investigative ophthalmology & visual science* 2007;48(5):2297-303.
8. McCarey BE, Edelhauser HF, Lynn MJ. Review of corneal endothelial specular microscopy for FDA clinical trials of refractive procedures, surgical devices, and new intraocular drugs and solutions. *Cornea* 2008;27(1):1-16.
9. Del Priore LV, Kuo YH, Tezel TH. Age-related changes in human RPE cell density and apoptosis proportion in situ. *Investigative ophthalmology & visual science* 2002;43(10):3312-8.
10. Panda-Jonas S, Jonas JB, Jakobczyk-Zmija M. Retinal pigment epithelial cell count, distribution, and correlations in normal human eyes. *American journal of ophthalmology* 1996;121(2):181-9.
11. Watzke RC, Soldevilla JD, Trune DR. Morphometric analysis of human retinal pigment epithelium: correlation with age and location. *Current eye research* 1993;12(2):133-42.
12. Harman AM, Fleming PA, Hoskins RV, et al. Development and aging of cell topography in the human retinal pigment epithelium. *Investigative ophthalmology & visual science* 1997;38(10):2016-26.
13. Dorey CK, Wu G, Ebenstein D, et al. Cell loss in the aging retina. Relationship to lipofuscin accumulation and macular degeneration. *Investigative ophthalmology & visual science* 1989;30(8):1691-9.
14. Ts'o MO, Friedman E. The retinal pigment epithelium. 3. Growth and development. *Archives of ophthalmology* 1968;80(2):214-6.
15. Gao H, Hollyfield JG. Aging of the human retina. Differential loss of neurons and retinal pigment epithelial cells. *Investigative ophthalmology & visual science* 1992;33(1):1-17.
16. Schneider CA, Rasband WS, Eliceiri KW. NIH Image to ImageJ: 25 years of image analysis. *Nature methods* 2012;9(7):671-5.

17. Linkert M, Rueden CT, Allan C, et al. Metadata matters: access to image data in the real world. *The Journal of cell biology* 2010;189(5):777-82.
18. Carpenter AE, Jones TR, Lamprecht MR, et al. CellProfiler: image analysis software for identifying and quantifying cell phenotypes. *Genome biology* 2006;7(10):R100.
19. Doughty MJ. Concerning the symmetry of the 'hexagonal' cells of the corneal endothelium. *Experimental eye research* 1992;55(1):145-54.
20. Facts about Age-related Macular Degeneration. National Eye Institute; 2009. (http://www.nei.nih.gov/health/maculardegen/armd_facts.asp). (Accessed).
21. Nagai H, Kalnins VI. Normally occurring loss of single cells and repair of resulting defects in retinal pigment epithelium in situ. *Experimental eye research* 1996;62(1):55-61.
22. Young RW. Pathophysiology of age-related macular degeneration. *Survey of ophthalmology* 1987;31(5):291-306.
23. Kopitz J, Holz FG, Kaemmerer E, et al. Lipids and lipid peroxidation products in the pathogenesis of age-related macular degeneration. *Biochimie* 2004;86(11):825-31.
24. de Jong PT. Age-related macular degeneration. *The New England journal of medicine* 2006;355(14):1474-85.
25. Beatty S, Koh H, Phil M, et al. The role of oxidative stress in the pathogenesis of age-related macular degeneration. *Survey of ophthalmology* 2000;45(2):115-34.
26. Perron M, Harris WA. Retinal stem cells in vertebrates. *BioEssays : news and reviews in molecular, cellular and developmental biology* 2000;22(8):685-8.
27. Tropepe V, Coles BL, Chiasson BJ, et al. Retinal stem cells in the adult mammalian eye. *Science* 2000;287(5460):2032-6.
28. Heron M. Deaths: leading causes for 2010. *National vital statistics reports : from the Centers for Disease Control and Prevention, National Center for Health Statistics, National Vital Statistics System* 2013;62(6):1-97.
29. Van Meter WS, Katz DG, White H, et al. Effect of death-to-preservation time on donor corneal epithelium. *Transactions of the American Ophthalmological Society* 2005;103:209-22; discussion 22-4.
30. Chew EY, Lindblad AS, Clemons T. Summary results and recommendations from the age-related eye disease study. *Archives of ophthalmology* 2009;127(12):1678-9.

TABLES / FIGURES

Table 1: Summary of Past Studies

Study Authors	Sample Size	Cells	Areas of Retina	Measurements	Methods	Study Findings
Ts'o and Friedman (1968)	10 eyes	RPE	5 concentric regions around the macula	Cell density Cell area	RPE flatmounts were bleached; cells counted manually; cell area determined by dividing the total retinal area by # of cells	<ul style="list-style-type: none"> - RPE cell density decreases in the posterior pole with age - equatorial RPE cell density increased with age cell area decreased with age in posterior pole, increased in equator and periphery
Dorey et al. (1989)	30 eyes	PR RPE	Macula Paramacula Equatorial	Cell density	Fixed and embedded eyes; cells counted manually from radial sections	<ul style="list-style-type: none"> - RPE density decreased in posterior pole; not quantified - No changes with age in equator
Gao and Hollyfield (1992)	35 eyes	GC PR RPE	Fovea Peripheral Retina	Cell Density	Tissue was embedded and sectioned; cells counted by one observer	<ul style="list-style-type: none"> - No age related changes in foveal RPE cell density - Peripheral RPE loss 14 cells/mm²/year - RPE density = 5531 - 14 X age (years), Foveal RPE density 63% higher than periphery
Watzke et al. (1993)	20 eyes	RPE	Fovea Temporal Posterior pole Peripheral retina	Cell density Cell area Form factor Polymegathism	RPE flatmounts were bleached; cells counted manually	<ul style="list-style-type: none"> - no age effect on cell density or cell area found in any of the regions - RPE cells of fovea and temporal posterior pole were more hexagonal in younger eyes
Panda-Jonas et al. (1996)	53 eyes	PR RPE	Fovea Mid-periphery Outer-periphery	Cell Density	25 biopsy specimens of the retina and RPE; Cells were counted from photographs	<ul style="list-style-type: none"> - Total RPE cell density decreased by 0.3% per year - fovea (4,220 ± 727 cells/mm²) - mid-periphery (3,002 ± 460 cells/mm²) - outer periphery (1,600 ± 411 cells/mm²)
Harman et al. (1997)	38 eyes	RPE	Whole Retina	Cell Density	Wholemouted RPE; cells counted by manual tracing	<ul style="list-style-type: none"> - No age effect on cell density found in any regions of retina
Del Priore et al. (2002)	22 eyes	RPE	4 concentric regions around the fovea	Cell Density # Apoptotic cells	RPE flatmounts were TUNEL stained and counted	<ul style="list-style-type: none"> - Total RPE cell density decreased by 0.23% per year - RPE density (cells/mm²)= 4,890 x 11.3 (age) - Significant change in the density of RPE cells only seen in Zone 4

						<ul style="list-style-type: none">- Cell density decreased in the RPE w/increased distance from fovea- Zone 1 (4980 ± 90 cells/mm²); Zone 2 (4857 ± 75 cells/mm²); Zone 3 (4068 ± 207 cells/mm²); Zone 4 (4024 ± 137 cells/mm²)
--	--	--	--	--	--	--

RPE= Retinal Pigment Epithelium

PR= Photoreceptors

GC= Ganglion Cell

TUNEL= Terminal deoxynucleotidyl transferase dUTP nick end labeling

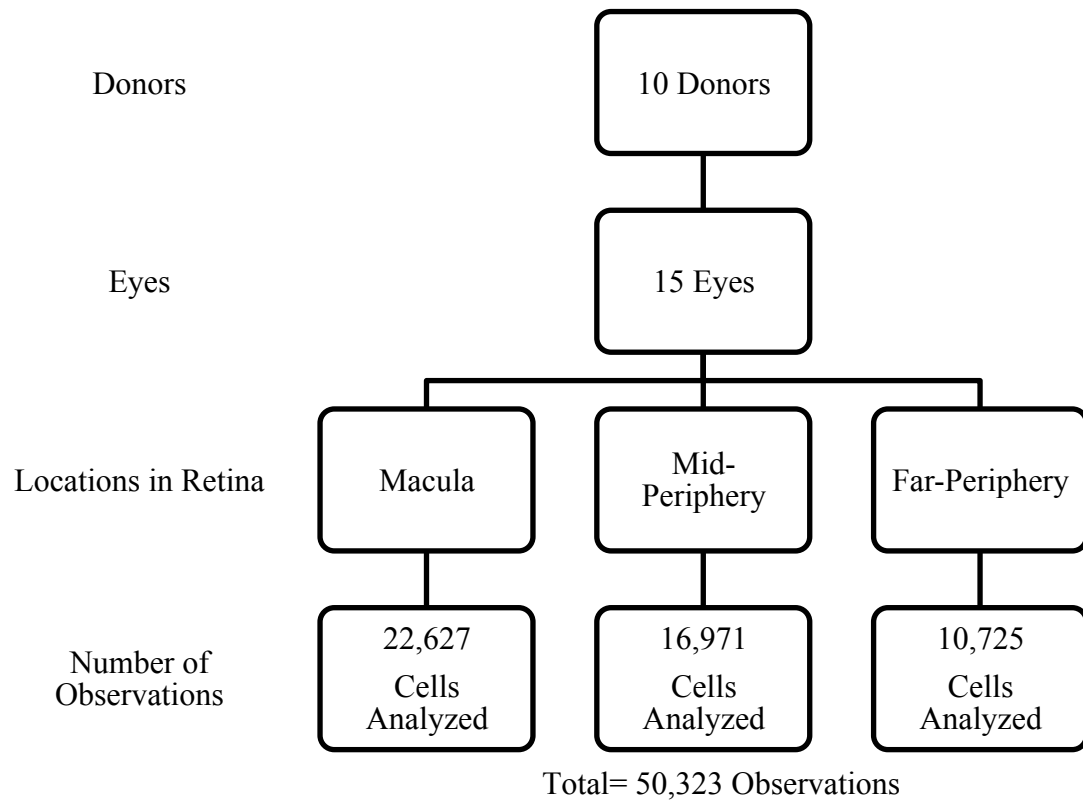


Figure 1: Study Population Diagram

A total of 10 donors were used in this study. For some donors, both left and right eyes were used for analysis. Three locations of the retina were analyzed for each donor eye: the macula, mid-periphery and far-periphery.

Table 2: Donor Characteristics

Age	Race	Sex	Cause of Death	Ocular history	Death to Preservation Time (hrs)	# of Eyes Used
29	White	M	Unknown	None noted	Not determined	2
37	White	F	Stroke	Wore glasses	0.65	2
42	White	M	GI bleeding	None noted	5.76	1
54	White	F	Ovarian Cancer	None noted	6.53	1
62	White	M	Pancreatic Cancer	None noted	4.80	1
67	White	F	Breast Cancer	None noted	2.95	1
71	White	F	Lung Cancer	Retinal det, cataract	6.48	2
71	White	M	Brain Cancer	None noted	3.78	2
75	White	M	Unknown	None noted	3.86	2
80	White	M	Bladder Cancer	None noted	4.00	1

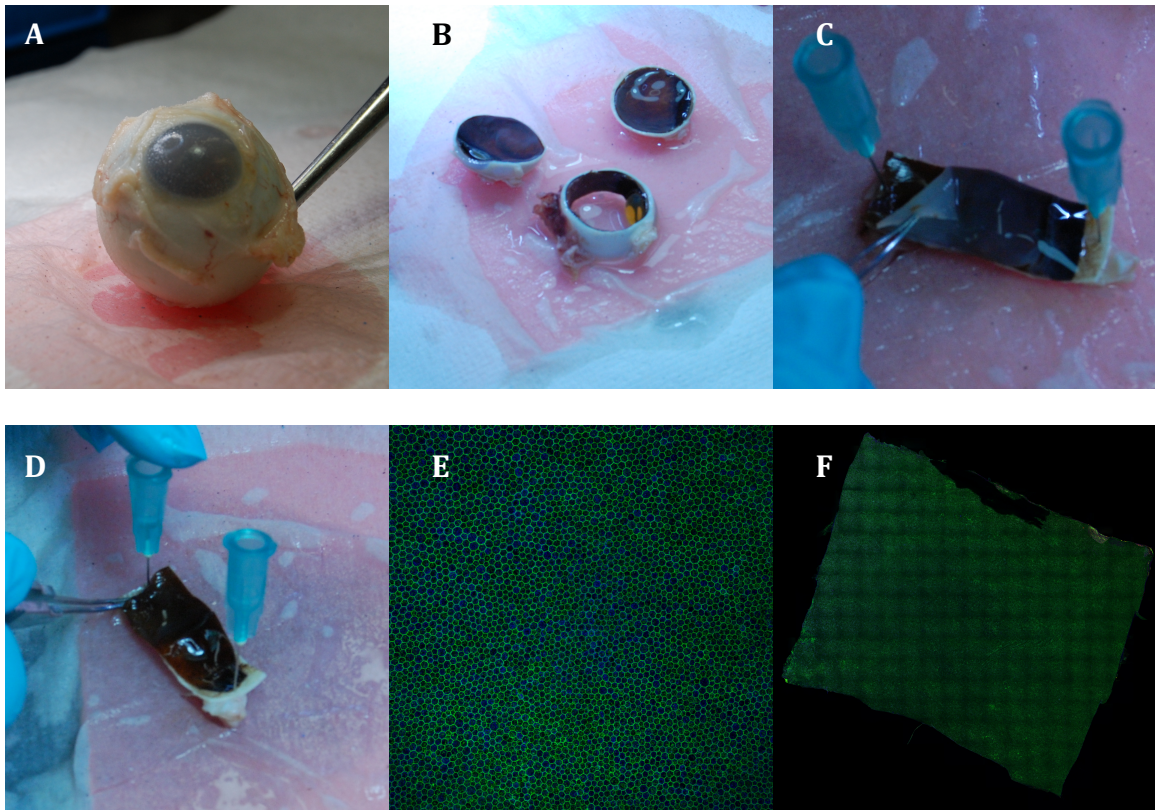


Figure 2: Description of Methods

Whole eyes were received from the eye bank (A). Globes were divided superiorly and inferiorly (B). Strip containing optic nerve and ciliary body was trimmed and neurosensory retina was peeled off (C). RPE and Bruch's membrane were gently dissected off of the sclera (D). Tissue was stained and imaged with confocal microscopy (E). Individual images were stitched together resulting in a composite image (F).

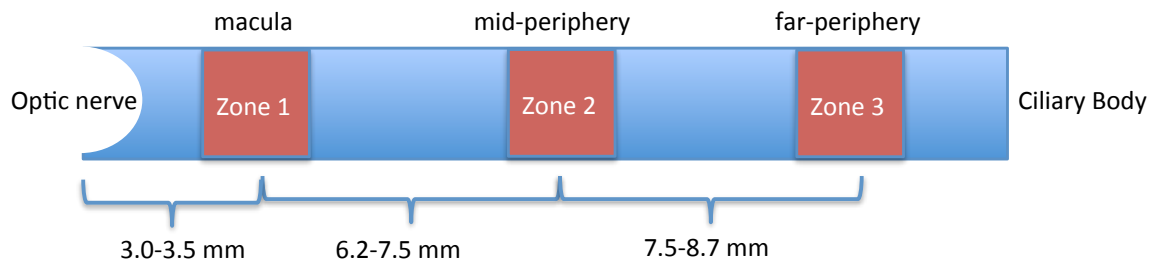


Figure 3: Image Selection

A total of 9 images were selected for analysis from each donor eye. Three images were selected from each of the above zones. Zone 1 corresponded to the macula, identified as the area 3.0-3.5 mm from the optic nerve and the area of the retina with the highest RPE cell density. Zone 2 corresponded to the mid-periphery, which was measured to be 6.2-7.5 mm from Zone 1. Zone 3 corresponded to the far-periphery, which was measured to be 7.5-8.7 mm from the mid-periphery.

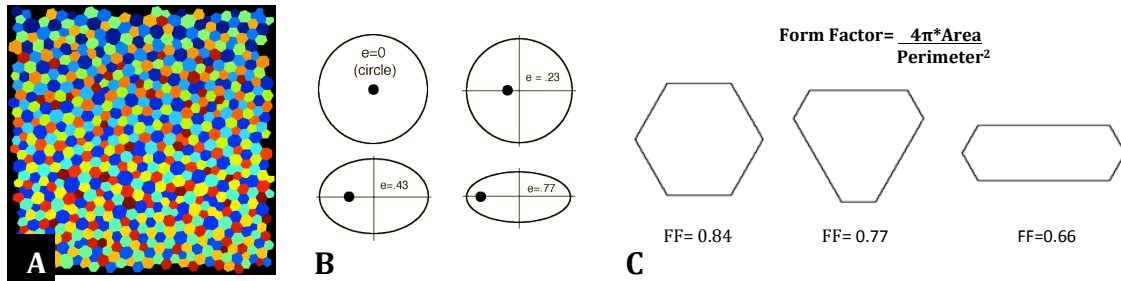


Figure 4: Image Analysis Technique

An image analysis software was used to automatically trace cell borders from individual images (A). Eccentricity, a measure of cell shape was recorded for each individual cell. A higher value corresponded to a more elongated shape (B). Form factor was calculated for each cell as the ratio of the cell's area to its perimeter squared. The form factor value for a perfect equilateral hexagon was 0.84. A lower form factor value corresponded to a cell that resembled an equilateral hexagon less.

Table 3: Descriptive Statistics of RPE Morphometric Measurements

	Macula	Mid-Periphery	Far-Periphery
Cell Density			
Average (SD)	4964.52 (1039.55)	3989.53 (521.51)	2521.22 (907.88)
Median (IQR)	4966.28 (1184.80)	4176.41 (450.88)	2290.61 (1515.55)
Cell Area			
Average (SD)	177.34 (81.67)	215.39 (88.44)	328.62 (162.82)
Median (IQR)	158.41 (86.93)	197.82 (90.22)	285.91 (176.95)
Eccentricity			
Average (SD)	0.51 (0.16)	0.55 (0.15)	0.63 (0.15)
Median (IQR)	0.50 (0.19)	0.54 (0.20)	0.65 (0.20)
Form Factor			
Average (SD)	0.76 (0.09)	0.75 (0.08)	0.74 (0.08)
Median (IQR)	0.78 (0.07)	0.77 (0.07)	0.76 (0.07)
% Hexagonal Cells			
Average (SD)	40.17 (4.42)	38.51 (3.69)	39.40 (5.00)
Median (IQR)	39.50 (3.71)	38.78 (3.43)	41.24 (4.06)

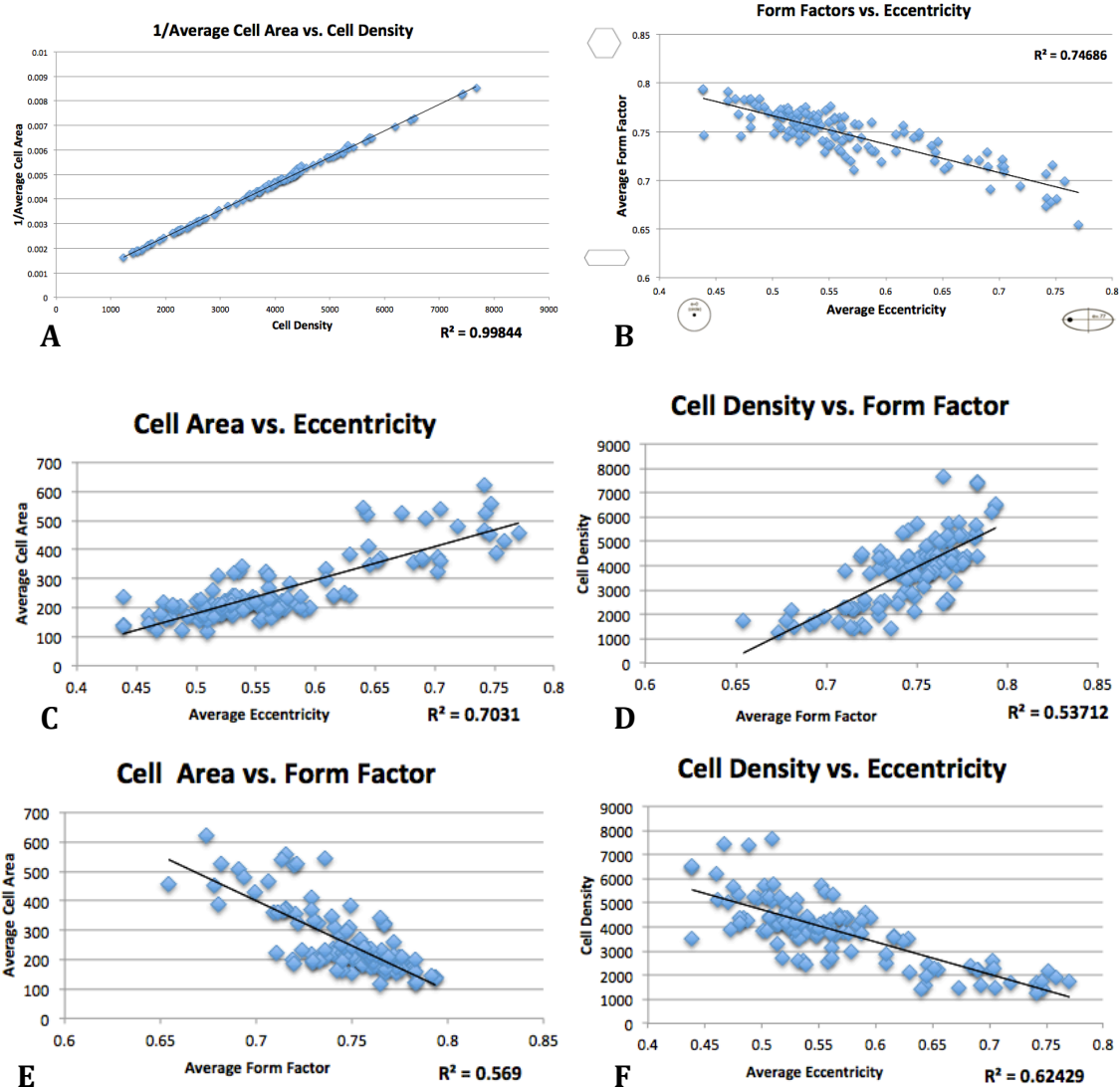


Figure 5: Correlation Analysis

There is a perfect correlation between 1/average cell area and cell density, and a strong negative correlation between average form factor and average eccentricity, confirming integrity of our dataset (A and B). There were positive correlations between average cell area and average eccentricity as well as cell density and average form factor (C and D). Negative correlations exist between average cell area and form factor, and cell density and average eccentricity (E and F).

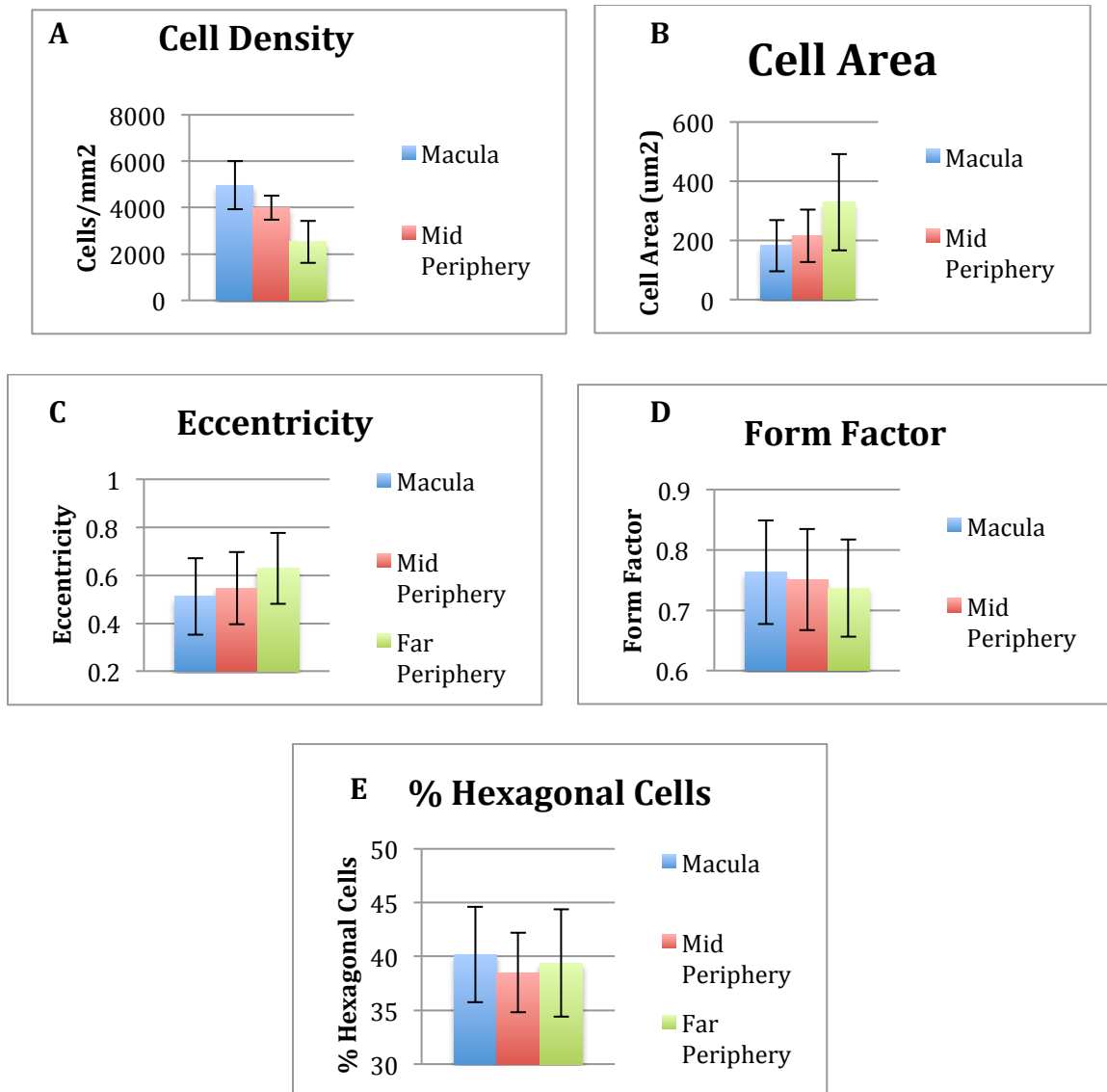


Figure 6: Analysis of Spatial Variation of RPE Morphometry

Average cell density (A), average cell area (B), average eccentricity (C), average form factor (D) and average percentage of hexagonal cells (E) are across all ages groups in three areas of the retina. Error bars represent standard deviations.

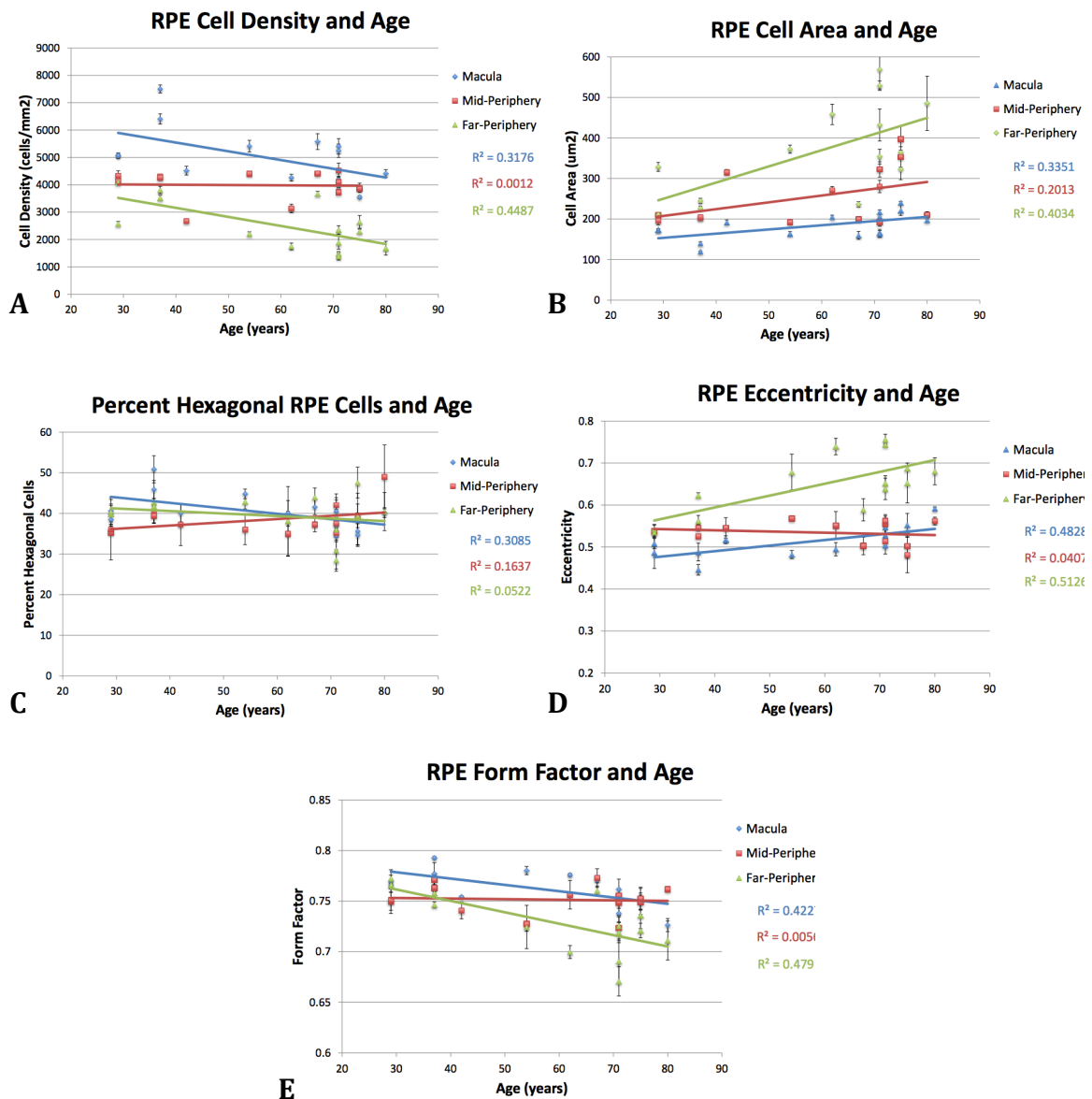


Figure 7: Composite Graphs Showing Age-Related Morphometric Changes of RPE in all 3 Areas of Retina

Various morphometric measurements from three areas of the retina are plotted against age. Each point on the graph represents an average of measurements taken from three images from a single donor. The error bars represent the standard deviation of those three measurements.

Table 4: Average Morphometric Measurements Comparing Patients <60 Years and ≥60 Years of Age

	Measurement	Average <60 years	Average ≥60 years	p-value*
Macula	Cell Density	5662.35	4499.31	0.03
	Cell Area	160.37	197.48	0.02
	Eccentricity	0.49	0.5315	0.01
	Form Factor	0.77	0.7528	0.03
	% Hexagonal Cells	43.46	37.98	0.01
Mid-Periphery	Cell Density	4014.60	3823.90	0.57
	Cell Area	219.93	219.47	0.98
	Eccentricity	0.54	0.53	0.36
	Form Factor	0.75	0.75	0.78
	% Hexagonal Cells	37.278	39.33	0.30
Far-Periphery	Cell Density	3235.82	2124.23	0.02
	Cell Area	276.74	416.80	0.02
	Eccentricity	0.59	0.6821	0.01
	Form Factor	0.75	0.7149	0.01
	% Hexagonal Cells	41.50	38.24	0.26

* $\alpha=0.05$, significant p-values marked in bold

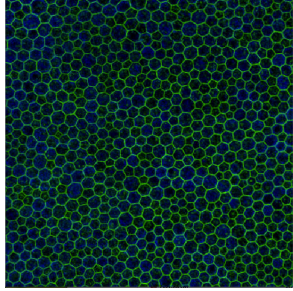
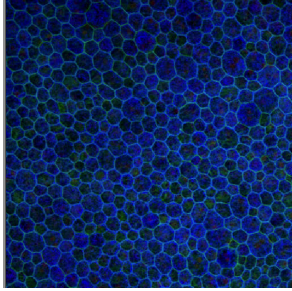
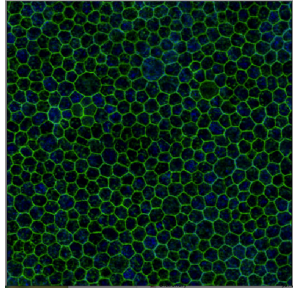
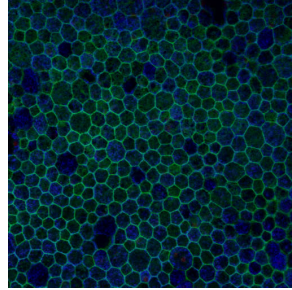
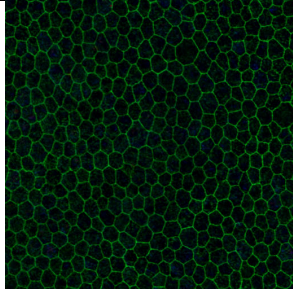
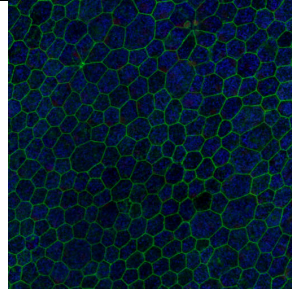
	Young (Age<60 years)	Old (Age≥60 years)
Macula		
Mid-Periphery		
Far-Periphery		

Figure 8: Representative Images of RPE Flatmounts

Representative images comparing a “young” donor (37 years old) to an “old” donor (75 year old) are shown here. When compared to the young donor, the old donor’s cells appear to be larger, elongated and more polymorphic.

Variable	Parameter Estimate	Standard Error	t Value	Pr > t (p value)	Variance Inflation Factor
Intercept	133.22	1.05	126.51	<0.0001	0
Cell Density	-0.009	0.0001	-74.48	<0.0001	1.94
Cell Area	-0.02	0.001	-17.85	<0.0001	6.91
Eccentricity	74.14	1.63	45.36	<0.0001	7.92
Form Factor	-55.15	2.30	-23.96	<0.0001	4.55
Number of Neighbors	-2.99	0.29	-10.38	<0.0001	11.28
R ² = 0.38, Root MSE= 14.01, Median of 95% prediction interval= 57.51 years					

Table 5: Linear Regression Model Parameter Estimates

A linear regression model was developed using data of morphometric measurements from the macula. The outcome variable was “RPE age” and the predictor variables were cell density, cell area, eccentricity, form factor and number of neighbors.